JOURNAL OF CATALYSIS 120, 256–271 (1989)

Multiple Reaction States in CO Hydrogenation on Alumina-Supported Cobalt Catalysts

WON H. LEE[1] AND CALVIN H. BARTHOLOMEW[2]

BYU Catalysis Laboratory, Department of Chemical Engineering, Brigham Young University, Provo, Utah 84602

Received April 17, 1989; revised July 10, 1989

CO hydrogenation was studied on four (1, 3, 10 and 15 wt%) Co/Al_2O_3 catalysts using the technique of temperature-programmed surface reaction (TPSR). Two distinct methane peaks (Peaks *A* and *B*) are observed for 3, 10 and 15% Co/Al_2O_3 during TPSR of chemisorbed CO at room temperature, indicating the presence of two different reaction states or mechanisms for CO hydrogenation (*A* and *B*). No methane peak is observed for 1% Co/Al_2O_3 unless it is reduced at 1023 K. The more active *A* state, the relative population of which increases with increasing metal loading and increasing extent of reduction, probably corresponds to hydrogenation of atomic carbon on 3*D* cobalt crystallites while the less active *B* state is assigned to decomposition on metal crystallites of a methoxy or formate species originally formed on the support from spilled-over hydrogen and carbon monoxide. TPSR spectra of hydrogen with carbon deposited by CO dissociation at 523 K show that the quantity of active α-carbon increases with increasing metal loading and correlates with the relative population of *A* sites. A linear correlation between logarithm of the steady-state methane turnover frequency and the relative population of *A* sites suggests that large variations in the steady-state CO hydrogenation rate with dispersion and metal loading observed for these catalysts may be explained in terms of variations in the distribution of reaction states for CO hydrogenation, i.e., a larger fraction of Reaction *A* at higher metal loadings and higher extents of reduction.

INTRODUCTION

Significant variations in CO hydrogenation activities of supported Group VIII metals with changes in dispersion and metal concentration have been observed by a number of laboratories (*1–11*). For example, the CO hydrogenation activity of Co/Al_2O_3 has been observed to vary over about 2–3 orders of magnitude depending upon preparation, dispersion, and metal loading (*5–8*). The origin of these variations is a matter of considerable interest and has stimulated a number of recent investigations (*8–15*). Several previous investigators (*2, 4, 6, 9*) have attributed these variations in activity with dispersion to changes in structure with changing metal crystallite size, i.e., to primary structure sensitivity. However, this hypothesis is not consistent with reaction studies on Co, Ru, and Ni single crystals (*15–19*), which provide strong evidence that CO hydrogenation activity on these metals is independent of surface structure. Accordingly, other causes such as metal–support interactions and activity modifications by unreduced metal oxides need to be more fully considered.

Indeed, it is well established that metal oxide–metal oxide and metal–metal oxide interactions play an important role in the chemistry of alumina-supported base metals (*5–8, 12, 13, 20–34*). For example, cobalt oxide interacts strongly with Al_2O_3 to form cobalt aluminate which is difficult to reduce (*20, 21, 24, 25*); the extent of such interaction is affected by metal loading, preparation, and pretreatment (*5, 13, 20, 24, 25*). Furthermore, the adsorption and activity/selectivity properties of Co/Al_2O_3

[1] Present address: Department of Chemical Engineering, University of Illinois, Urbana, IL 61801.

[2] To whom correspondence should be addressed.

0021-9517/89 $3.00

are greatly influenced by these same parameters (*5–8, 13, 22–25*). In other words, the catalytic properties of alumina-supported cobalt depend on the distribution of metallic cobalt and cobalt oxide species.

In fact, recent temperature-programmed surface reaction (TPSR) studies of hydrogen with adsorbed CO on alumina-supported Ni (*26–29, 33, 34*) provide evidence for the existence of two different kinds of active sites for CO hydrogenation, one associated with surface metal atoms surrounded by other metal atoms and one involving metal atoms or metal ions associated with the support (*26–29*) or involving the support itself (*33, 34*). However, it is also possible that the previous results (*26–29, 33, 34*) could be explained by two different reaction states (paths) rather than by two different sites.

The objectives of this study were (1) to identify, by means of hydrogen TPSR with adsorbed CO, active sites and/or reaction states for CO hydrogenation on Co/Al_2O_3; (2) to investigate the effects of metal loading and reduction pretreatment on distribution of these sites/states; and (3) to shed light on the origin of the apparent structure sensitivity in CO hydrogenation observed on Co/Al_2O_3 catalysts.

EXPERIMENTAL

Materials. Catalysts used in this study were prepared by incipient wetness impregnation of Dispal-M γ-Al_2O_3 (sample No. 8032H from Conoco) with an aqueous solution of $Co(NO_3)_2$ (*5*). After preparation, catalysts were oven-dried overnight at 373 K. The unsupported cobalt was prepared by heating $Co(NO_3)_2$ at 473 K overnight. Metal loading, extent of reduction, dispersion, and turnover frequencies for conversion of CH_4 during CO hydrogenation for these catalysts previously determined in this laboratory (*6, 7*) are summarized in Table 1.

All gases were ultrahigh purity grade (99.999%) from Matheson. Hydrogen was passed through a Pt/Pd oxygen-removal trap (Girdler Catalysts, Chemetron Corp.) and a molecular sieve (Linde Type 5A). Helium was passed successively over a molecular sieve, a heated copper Deoxo, and another molecular sieve. The adsorbate gas consisting of 10% CO in He was passed through a heated molecular sieve to remove carbonyls. For the exposure of the catalyst to oxygen, 10% O_2/He (from Matheson) was used without further purification.

TABLE 1

Metal Loading, Extent of Reduction, Dispersion, and Turnover Frequencies[a] of Co/Al_2O_3 Catalysts

Metal loading (%)	Extent of reduction (%)	D (%)	$N_{CO} \times 10^3$ at 225°C[b] (s^{-1})	$N_{CH_4} \times 10^3$ at 225°C[c] (s^{-1})
1	11	34	Inactive	Inactive
3	28	15	6.4	1.2
10	34	9.9	12	3.8
15	44	6.6	63	8.0
100	100	0.26	5.8	1.1

[a] Data for unsupported cobalt and 1, 3, 10, 15% Co/Al_2O_3 were taken from Reuel and Bartholomew for the same catalysts (*5*).

[b] Turnover frequency in molecules per hydrogen adsorption site per second for CO conversion.

[c] Turnover frequency for methane production.

Apparatus and procedure. The TPD/TPSR system incorporated an on-line quadruple mass spectrometer (UTI 100C). Details of the apparatus and data acquisition procedure are reported elsewhere (*23, 35*).

A powdered catalyst sample (20–100 mg) was placed in a quartz microreactor, the middle section of which was bulb-shaped to reduce the depth of catalyst bed and thereby minimize the temperature and concentration gradients along the bed (*23, 35*). The absence of pore diffusional effects, sample measurement lag time, and concentration gradients within each catalyst particle during reaction and desorption measurements was also established (*23, 35*). The reactor tube was housed inside a tubular nichrome-wire-wrapped quartz furnace which was resistively heated. The catalyst temperature, during experiments, was

monitored continuously by an unshielded chromel–alumel thermocouple which was placed directly in the catalyst bed. The second thermocouple was placed in contact with the furnace wall in the annular space between the furnce and the reactor to drive a temperature controller. A heating rate of 33 K/min was used for all runs.

Prior to a TPSR measurement, the sample was reduced in H_2 flowing at about 60 cm^3/min according to a reduction schedule including a temperature ramp of 3 K/min (from 298 K) with a 1-h hold at 373 K to facilitate water removal, a 1-h hold at 473 K to avoid the rapid nitrate decomposition, and 24 h at 648 K.

After reduction, the sample was purged in He for 15 min at 648 K and cooled to 298 K in flowing He. CO was adsorbed at 298 or 523 K by injecting a pulse (0.1 cc/pulse) of 10% CO/He into flowing He every 30 s for 10 min, the total quantity of which corresponded to several monolayers of CO. Ten minutes were allowed for the excess gas to be removed. The sample was then heated at 33 K/min from 298 K to 648 K in 60 cm^3/min of pure H_2. Effects of reduction temperature were studied on the same catalyst reduced initially at 648 K by reducing further at higher temperatures for 12 h at each temperature.

During the TPSR experiments, CH_4, CO, CO_2, and C_2H_6 were detected simultaneously by monitoring the mass signals (m/e) 15, 28, 44, and 30, respectively. The mass number of 15 instead of 16 was used for methane to avoid interference of water vapor and cracking of CO_2 and CO.

RESULTS

Hydrogenation of CO Preadsorbed at 298 K

Figure 1 shows the CH_4 TPSR spectra obtained for CO preadsorbed at 298 K on 1, 3, 10, and 15% Co/Al_2O_3 reduced at 648 K. The CH_4 TPSR spectrum for unsupported cobalt (reduced at 673 K) is shown by the dotted line for comparison. Each spectrum is plotted to a vertical scale to make the heights of the first CH_4 peak the same. A small amount of unreacted CO also desorbed at about 373 K during TPSR (not shown in Fig. 1).

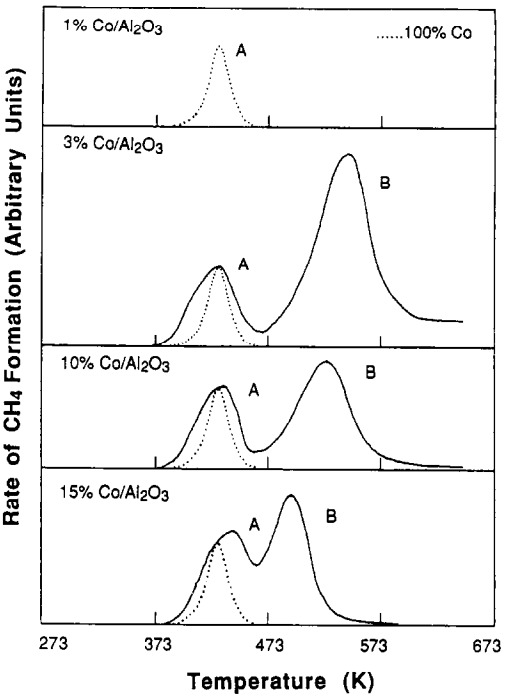

FIG. 1. CH_4 TPSR spectra for unsupported cobalt (shown as the dotted line) and Co/Al_2O_3 catalysts of different metal loadings. Co/Al_2O_3 catalysts were reduced at 648 K and CO was adsorbed at 298 K in He.

As shown in Fig. 1, two CH_4 peaks are observed for 3, 10, and 15% Co/Al_2O_3 (the low-temperature peak designated as *A* and the high-temperature peak as *B*) while no CH_4 peak is observed for 1% Co/Al_2O_3. For unsupported cobalt, only a single CH_4 peak is observed. While the position of Peak *A* is nearly independent of metal loading (shifts only slightly to higher temperature), it is evident that Peak *B* becomes narrower and shifts significantly to lower temperature with increasing metal loading. It is apparent that the area for Peak *B*, relative to that of Peak *A*, decreases with increasing metal loading. It is significant that the position of Peak *A* is very close to that observed for unsupported Co.

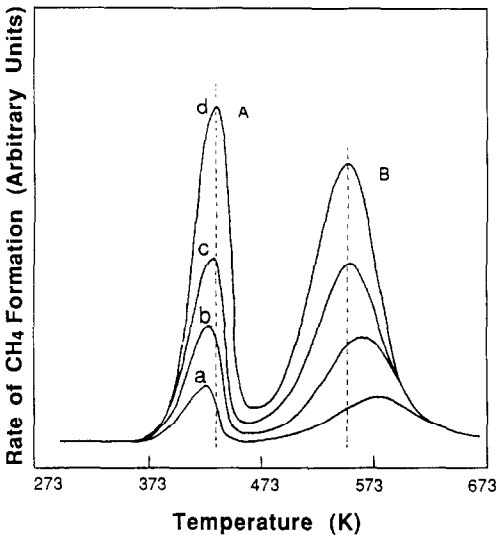

FIG. 2. CH_4 TPSR spectra for various CO initial coverages on 10% Co/Al_2O_3 reduced at 873 K: (a) θ = 0.18, (b) θ = 0.43, (c) θ = 0.67, (d) θ = 1.0 (CO adsorbed at 298 K in He).

TABLE 2

Activation Energies and Preexponential Factors[a,b,c] for Methane Peak *B* as Functions of Metal Loading and Reduction Temperature

Catalyst	Preexponential factor (s^{-1}) × 10^{-6} for various reduction temperatures (K)				E_{act} (kJ/mol)
	648	773	873	973	
3% Co/Al_2O_3	29	19	6.4	2.1	95 ± 3
10% Co/Al_2O_3	110	52	42		98 ± 2
15% Co/Al_2O_3	400	190	130		97 ± 2

[a] Activation energies were determined from Arrhenius plots and preexponential factors were determined from Redhead's formula (*36*).

[b] Activation energies and preexponential factors for Peak *A* are nearly independent of reduction temperature and metal loading (except for 1% Co/Al_2O_3): E_A = 81 ± 2 kJ/mol, $\nu_A = 1.7 \times 10^8\ s^{-1}$.

[c] For 1% Co/Al_2O_3 reduced at 1023 K, E_A = 101 ± 5 kJ/mol, $\nu_A = 1.93 \times 10^{10}\ s^{-1}$.

Typical CH_4 spectra obtained for various amounts of CO exposure are shown in Fig. 2. As initial CO coverage increases, Peak *A* shifts to higher temperature while Peak *B* shifts to lower temperature; however, the shift in the position of Peak *B* is more significant. The relative area for Peak *A* increases slightly with increasing initial CO coverage (about 0.33 for Spectra a and b, 0.34 for Spectrum c, and 0.38 for Spectrum d).

In Fig. 3, the CH_4 TPSR spectrum for CO chemisorbed at 298 K in flowing H_2 is compared with that for CO chemisorbed at 298 K in flowing He. The area under Peak *A* is slightly lower for the former while that for Peak *B* is significantly higher, indicating that CO adsorption is enhanced in the presence of H_2. No changes in peak temperatures are observed.

Table 2 summarizes Peak *B* activation energies and preexponential factors for TPSR of hydrogen with CO adsorbed at 298 K as a function of metal loading and reduction temperature. Activation energies were determined from the linear portions of Arrhenius plots of $\mathrm{Ln}[(-d\theta/dT)/\theta]$ vs $1/T$ while preexponential factors were calculated from Redhead's formula (*36*). Activation energies and preexponential factors for Peak *A* were found to be (with the exception of 1% Co) nearly independent of metal

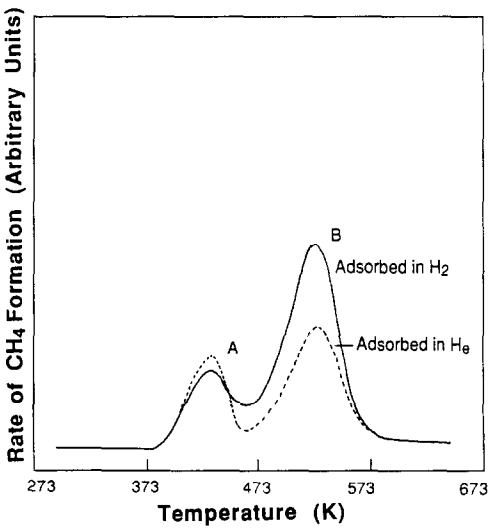

FIG. 3. CH_4 TPSR spectra for 10% Co/Al_2O_3 reduced at 648 K: (a) CO adsorbed at 298 K in H_2 (solid line), and (b) CO adsorbed at 298 K in He (dotted line).

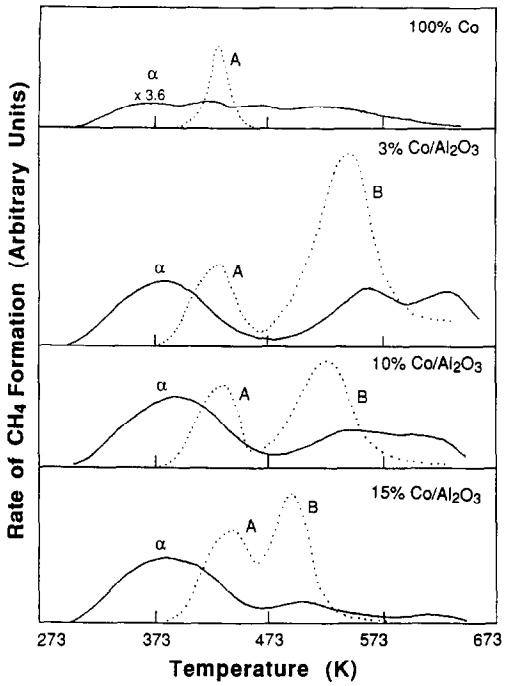

FIG. 4. CH_4 TPSR spectra for hydrogenation of carbon deposited by CO dissociation at 523 K (solid line) and for hydrogenation of CO adsorbed at 298 K (dotted line). All catalysts were reduced at 648 K (unsupported cobalt at 673 K).

loading with average values of $E_A = 81 \pm 2$ kJ/mol and $\nu_A = 1.7 \times 10^8\ s^{-1}$ ($E_A = 101 \pm 5$ kJ/mol, $\nu_A = 1.9 \times 10^{10}\ s^{-1}$ for 1% Co/alumina reduced at 1123 K). Preexponential factors for Peak *B* (Table 2) generally decrease with decreasing metal loading and increasing reduction temperature while activation energies are essentially independent of reduction temperature and metal loading for 3–15% Co.

Hydrogenation of CO Preadsorbed at 523 K

Figure 4 shows the CH_4 TPSR spectra for CO preadsorbed at 523 K on unsupported cobalt (reduced at 673 K) and on 3, 10, and 15% Co/Al_2O_3 catalysts reduced at 648 K. No methane peak was observed for 1% Co/Al_2O_3. The CH_4 spectra for CO preadsorbed at 298 K are shown as dotted lines for comparison. The scale for the CH_4 spectrum for unsupported cobalt after CO adsorption at 523 K is different from the rest of the spectra (smaller because of its lower surface area). The methane spectrum for CO adsorbed on unsupported cobalt at 523 K consists of several broad, overlapping methane peaks including a low-temperature peak at about 373 K and possibly a high-temperature peak at about 500 K. For the Co/Al_2O_3 catalysts, at least three CH_4 peaks are observed below 673 K: a broad, low-temperature peak from 273 to 473 K with a maximum at about 400 K and two high-temperature peaks at 473–600 K. The second methane peak appears within the range in which Peak *B* (shown as the second peak in dotted lines) is observed; its temperature peak position shifts to lower temperature with increasing metal loading, indicating that it may involve the same species as Peak *B* but at a low coverage. The third peak is observed at about 623 K for all catalysts. Data in Fig. 5 show that the relative area of the methane peak appearing at about 400 K assigned to α-carbon from CO dissociation (*37, 38*) increases linearly with increasing metal loading for Co/Al_2O_3 catalysts and is linearly correlated with the relative area for Peak *A* (first peak in the CH_4 spectra shown by the dotted lines in Fig. 4).

Effects of Reduction Temperature

Figure 6 shows effects of reduction temperature on the CH_4 spectra for 1, 3, and 15% Co/Al_2O_3 catalysts while Table 3 summarizes peak temperatures, peak areas (normalized with respect to those for 648 K reduction), and relative Peak *A* areas for all four Co/Al_2O_3 catalysts. Each spectrum in Fig. 6 was obtained after CO adsorption at 298 K following reduction of catalysts at the specified temperature. As indicated from the table, the relative area for Peak *A* increases with increasing metal loading at a given reduction temperature. Moreover, the fraction of *A* sites $[A/(A + B)]$ generally increases with increasing reduction temperature (although in the case of 15% Co/Al_2O_3

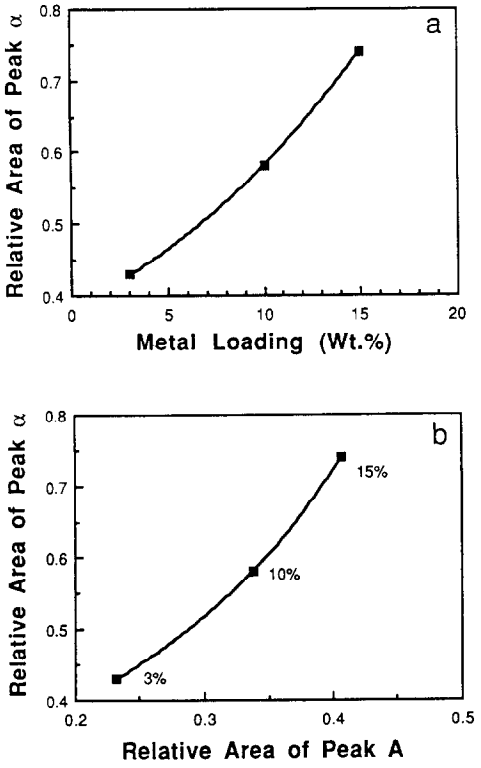

FIG. 5. (a) Relative Peak α areas (see Fig. 4) vs metal loading. (b) The relative area of Peak α (see Fig. 4) vs relative area of Peak *A* (see Fig. 1).

this fraction is the same written experimental error for all reduction temperatures).

No CH_4 peak is observed for 1% Co/Al_2O_3 when it is reduced at 873 K or below, although a CO desorption peak is observed at about 373 K. When the catalyst is reduced at 1023 K, however, two CH_4 peaks appear at about 447 and 723 K. For higher loading catalysts, two distinct CH_4 peaks are observed for reduction temperatures from 628 to 973 K, the areas of which increase with increasing reduction temperature (see Table 3). For a given catalyst Peak *B* shifts to higher temperature with increasing reduction temperature while the position of Peak *A* remains nearly constant; moreover, at a given reduction temperature, the position of Peak *B* is found at a progressively lower temperature with increasing metal loading.

Oxygen Exposure and Interrupted Experiments

Figure 7 shows the CH_4 spectrum obtained after 3% Co/Al_2O_3 (reduced at 973 K) was exposed to 10% O_2/He at 298 K followed by CO adsorption at 298 K. The spectrum shown by the dotted line was obtained after CO adsorption at 298 K on the reduced catalyst in the absence of oxygen exposure. Peak *A* disappears after oxygen exposure while Peak *B* survives although the area and the peak width decrease. For unsupported cobalt, no methane peak was oberved after oxygen exposure.

Two different interrupted experiments were conducted on 3% Co/Al_2O_3 reduced at 973 K. In the first experiment (Fig. 8), the experiment was interrupted by cooling the catalyst to 298 K rapidly in flowing H_2 when the catalyst temperature reached 473 K during TPSR. The spectrum shown by the dotted line was obtained prior to interrup-

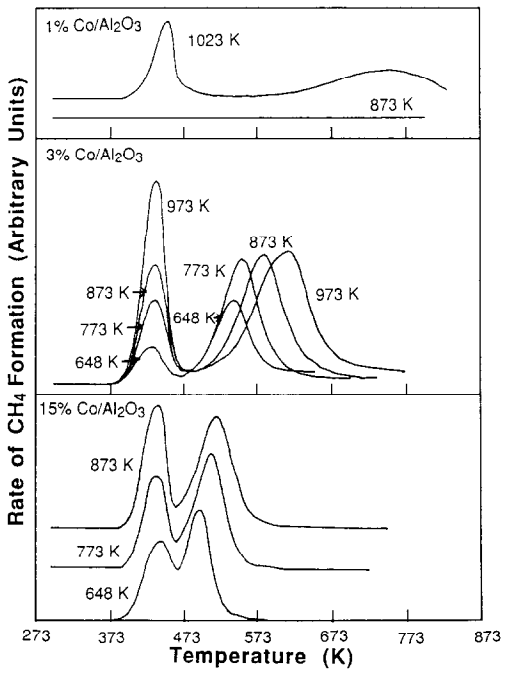

FIG. 6. Effects of reduction temperature on CH_4 TPSR spectra. Reduction temperatures are specified. CO was chemisorbed at 298 K.

TABLE 3

Methane Peak Temperatures, Areas, and Area Ratios as Functions of Metal Loading and Reduction Temperature[a]

Catalysts and reduction temp. (K)	Peak temp. (K)		Peak area[b]		Peak area ratio[c] $A/(A+B)$
	A	*B*	*A*	*B*	
1% Co/Al_2O_3					
1023	447	757	1	1	0.42
3% Co/Al_2O_3					
648	432	543	1	1	0.23
773	432	553	2.17	1.57	0.29
873	432	581	3.31	2.26	0.30
973	432	613	4.79	2.46	0.37
10% Co/Al_2O_3					
648	432	526	1	1	0.34
773	432	543	2.06	2.12	0.33
873	432	548	3.12	2.61	0.38
15% Co/Al_2O_3					
648	440	494	1	1	0.41
773	434	509	1.22	1.19	0.38
873	434	517	1.47	1.29	0.40

[a] Based on the CH_4 TPSR for CO adsorbed at 298 K.
[b] Methane peak areas normalized with respect to those for 648 K reduction (except for 1% Co/Al_2O_3).
[c] Ratio of the area of Peak *A* to the sum of areas for Peaks *A* and *B*.

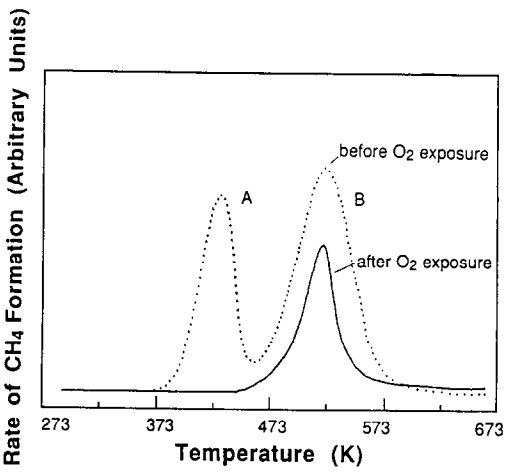

FIG. 7. The CH_4 TPSR spectrum obtained for CO adsorption after 3% Co/Al_2O_3 reduced at 973 K was exposed to oxygen at room temperature (solid line). Dotted line represents a typical CH_4 spectrum without oxygen exposure.

tion. Following this interruption, the catalyst temperature was raised from 298 K in flowing H_2 as a typical TPSR run to obtain the CH_4 peak shown by the solid line in Fig. 8. The combined spectrum of these two peaks is almost identical to that obtained during a normal TPSR run without an interruption. When the catalyst was cooled rapidly to 298 K in flowing He, the same result was obtained.

In the second experiment (Fig. 9), the TPSR run was interrupted at several temperatures and the catalyst was rapidly cooled to 298 K in flowing H_2. Then, the carrier gas was switched from H_2 to He and temperature-programmed desorption (TPD) was conducted in flowing He to obtain the spectra in Fig. 9. When the interruption takes place at 373 K followed by TPD, a significant quantity of CO (not determined quantitatively) desorbs and several peaks due to molecularly adsorbed CO and recombination of C_a and O_a are observed (bottom spectrum in Fig. 9a). However, as the interruption temperature increases, CO desorption peaks, appearing

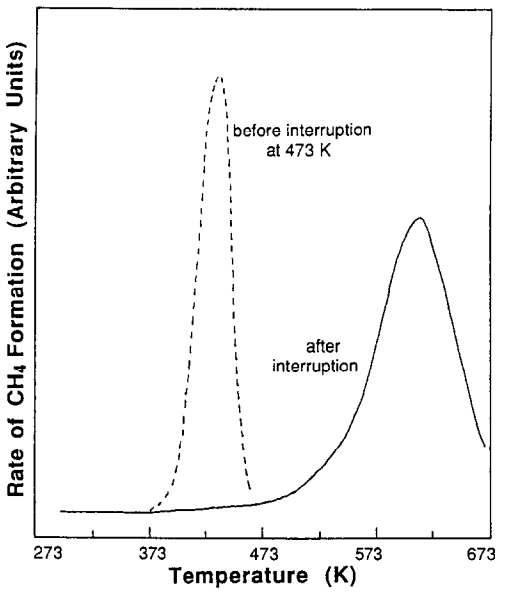

FIG. 8. CH_4 TPSR spectrum before and after interruption for 3% Co/Al_2O_3 reduced at 973 K. Dotted line represents the CH_4 spectrum obtained before interruption. Solid line represents the spectrum obtained after interruption.

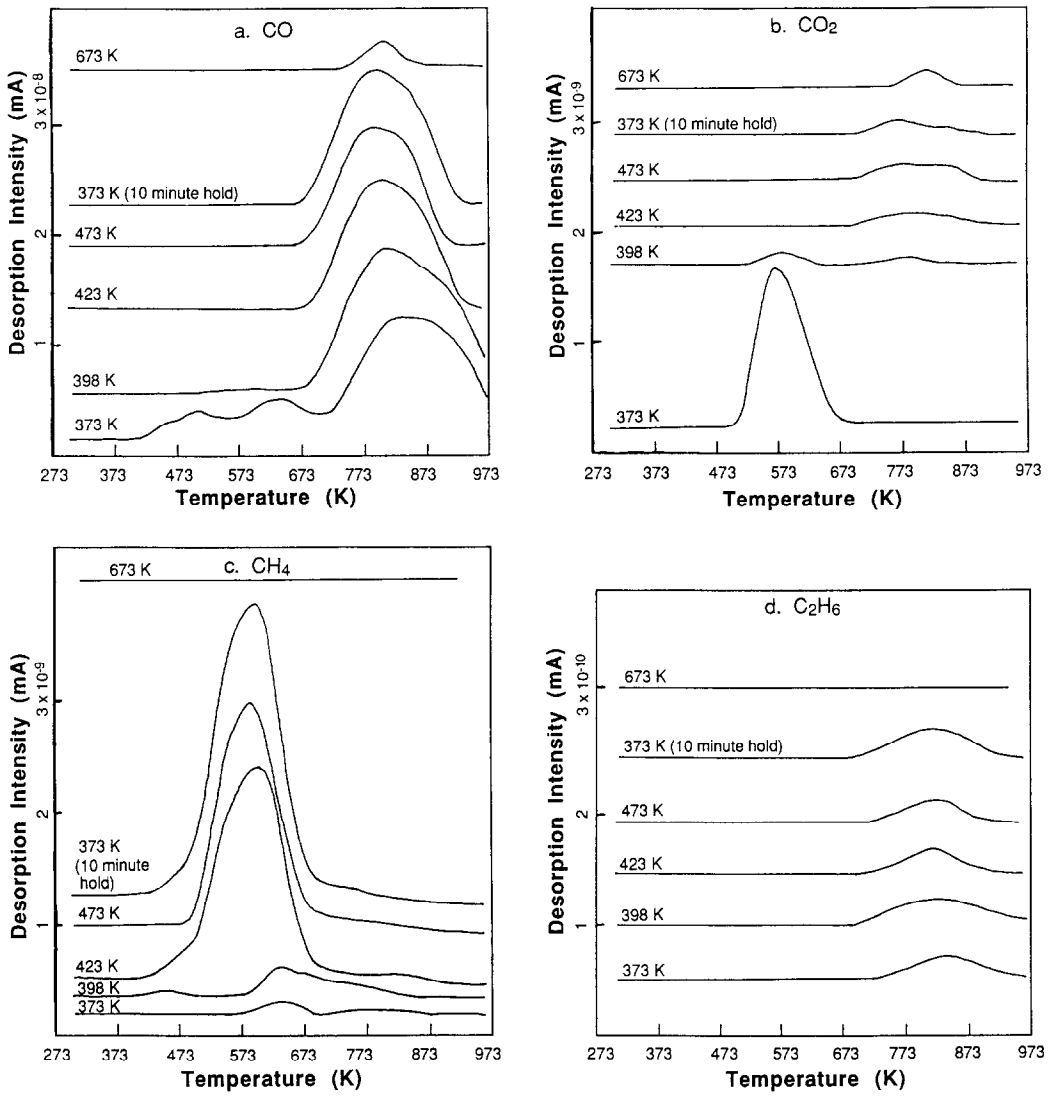

FIG. 9. TPD spectra obtained for 3% Co/Al_2O_3 reduced at 973 K after interruption during TPSR (interruption temperatures are specified): (a) CO, (b) CO_2, (c) CH_4, and (d) C_2H_6.

below 673 K due to molecularly adsorbed CO, vanish. After the interruption takes place at 423 K or above, only a broad high-temperature CO desorption peak is observed at above 773 K. For the case of interruption at 373 K with a 10-min hold, only a high-temperature CO peak is observed, indicating that most molecularly adsorbed CO species disappear during the 10-min hold at 373 K.

Significant desorption of CO_2 is also observed during TPD following interruption at 373 K (Fig. 9b). The peak temperature is about 573 K. However, this CO_2 peak disappears at higher interruption temperatures, which is also indicative of depletion of molecular CO on the surface.

Figure 9c shows the corresponding CH_4 spectra obtained during TPD. When the interruption takes place at 373 K, a small methane peak is observed at about 643 K. The area under the methane peak increases

rapidly with increasing interruption temperatures from 373 to 423 K. Ethane desorption is observed only at high temperatures (at about 823–833 K) for all interruption temperatures and its intensity is significantly lower compared with other desorbing species.

DISCUSSION

The results of this study provide new insights into the kinetics and mechanism of CO hydrogenation on alumina-supported cobalt. They show that the reaction involves two different states of different activities having properties very similar to those observed for Ni/Al_2O_3 (*26–29, 33, 34*). The results of this study also provide new evidence that CO hydrogenation on cobalt metal sites occurs either through dissociation to an active carbon followed by hydrogenation of the carbon or by decomposition of a species formed on the support. Finally, the results provide for the first time a satisfying explanation for previously observed variations in activity with dispersion and metal loading and provide further evidence that CO hydrogenation on cobalt is not structure-sensitive. A discussion of each of these points follows below.

The Nature of Active Sites on Co/Alumina

The results of hydrogen TPSR with CO adsorbed on Co/Al_2O_3 at 298 K from this study indicate two methane reaction states, *A* at 440 ± 7 K, the position of which is relatively invariant with metal loading or reduction temperature, and *B* at 500–973 K, the position of which is highly dependent upon metal loading and reduction temperature. These reaction states are very similar to those reported for hydrogen TPSR with adsorbed CO on Ni/Al_2O_3 (*26–29, 33, 34*); in fact, the reaction states observed in this study for 3% Co/Al_2O_3 at 432 and 543 K are very close to those observed by Kester and Falconer (*26*) for 3–5% Ni/Al_2O_3 at 446 and 546 K. Moreover, most of the qualitative observations regarding the effects of metal loading and reduction temperature as well as the quantitative measurements of reaction kinetics for Co/Al_2O_3 (this study) and Ni/Al_2O_3 (*26, 27*) are in good agreement. For example, in both systems the *A*/*B* peak area ratio increases with increasing metal loading and extent of reduction; in the Co/Al_2O_3 system the fraction under Peak *A* increases from zero for 1% Co to 0.4 for 15% Co whereas in the Ni/Al_2O_3 system the *A* fraction increases from 0.23 for 1.8% Ni to 0.93 for 15% Ni (*27*). In both catalyst systems the position of Peak *B* shifts very significantly to higher temperatures with decreasing metal loading and increasing reduction temperature; the area of Peak *B* is also increased in both systems by adsorbing or cooling in H_2 rather than He. Activation energies for Reaction *B* on 3% Ni/Al_2O_3 and 3% Co/Al_2O_3 are approximately the same within experimental error, i.e., 145 ± 39 (*26*) compared to 95 ± 3 kJ/mol (see Table 2).

The assignment of Peaks *A* and *B* to two different reaction *states* of differing rates is consistent with the data of this study and is supported by the data in previous studies of Ni/Al_2O_3 (*26–29, 33, 34*). However, in the previous studies Peaks *A* and *B* were assigned to two different reaction *sites*. The *A* sites were assigned to CO adsorbed on Ni metal atoms bonded to other Ni atoms (*26–29*). A similar assignment of the *A* state for Co/Al_2O_3 to hydrogenation of CO adsorbed on Co metal atoms bonded to other Co atoms, e.g., Co atoms in large, three-dimensional (*3D*) crystallites, is consistent with the results of this study; indeed, this is strongly supported by the observation from this study that only Peak *A* is observed on the completely reduced, unsupported Co catalyst (see Fig. 1) which consists entirely of large, *3D* Co metal crystallites. Furthermore, the complete disappearance of Peak *A* for the unsupported Co and Co/Al_2O_3 catalyst upon exposure to oxygen at 298 K provides further evidence for the strongly metallic nature of the sites for Reaction *A*.

Finally, the absence of both Peaks *A* and *B* on 1% Co/alumina (reduced below 1023 K), which nevertheless contains small crystallites that absorb both hydrogen and carbon monoxide (the latter only associatively), provides further evidence that large cobalt crystallites are a requirement for Reaction *A*.

On the other hand, the observation of Peak *B* for TPSR on Co/Al_2O_3 catalysts but not on unsupported Co coupled with the partial survival of Peak *B* after 298 K exposure to oxygen suggests that Reaction *B* involves species created on sites in the presence of the support and having chemical properties distinct from those of the *A* sites.

In previous studies of Ni/Al_2O_3 the *B* Peak was assigned to reactions of hydrogen with CO adsorbed on (1) surface nickel metal atoms interacting with an oxide phase of the catalyst (*26, 27*), (2) a surface nickel aluminate (*28, 29*), or (3) the Al_2O_3 support (*33, 34*). While selected sets of data in these previous studies provide some support for each of these three models, none appears in our opinion completely consistent with all of the data. Recent studies by Falconer *et al.* (*34*) of hydrogen TPSR with isotopes of CO on 5 and 19% Ni/Al_2O_3 catalysts provide evidence for the third model; their results show that (1) adsorption on the *B* sites is activated, (2) *B* sites are only saturated in the presence of hydrogen by increasing the adsorption temperature to 385 K (saturation coverage of 250 μmol/g catalyst for both catalysts), (3) the number of *B* sites is about four times that of the *A* sites in both catalysts, (4) after adsorption at 300 K and TPSR to 460 K to remove the *A* peak, cooling in He causes some of the labeled CO on the *B* sites to transfer to *A* sites, and (5) the stoichiomery for the complex adsorbed on the support is CH_3O. These results combined with those of TPSR/IR studies of Ni/Al_2O_3 (*33, 39*) were interpreted (*34*) as evidence that (1) *B* sites are present on the Al_2O_3 support, (2) CO and hydrogen on nickel crystallites (*A* sites) spill over to Al_2O_3 sites to form adsorbed methoxy radicals, and (3) the *B* peak is attributed to hydrogenation/decomposition of the adsorbed methoxy to methane.

It is our view that the data of this and previous studies are most consistent with a variation of this third model, namely one in which CO and hydrogen adsorb on metal crystallites (*A* sites) and spill over to the Al_2O_3 support where they form a methoxy (CH_3O) or formate intermediate; the methoxy or formate complex (henceforth referred to as CH_xO) then diffuses back to a metal crystallite where it decomposes to methane. In other words we propose that the data are explained by the existence of two *reaction states* (mechanisms or paths) rather than two different reaction sites. The support for this point of view is as follows:

1. It is generally accepted (*40*) that CO hydrogenation occurs readily on metal atoms having the ability to dissociate hydrogen and CO. Experiments as part of this (*35*) and a previous study (*41*) indicate that cobalt and nickel aluminates and high-surface-area aluminas are not active for CO hydrogenation. Cobalt and nickel aluminates do not adsorb CO or hydrogen (*35, 41, 42*). Adsorption of CO on Al_2O_3 is weak, nondissociative, and small relative to that on the metals under the conditions of the TPSR experiment (*35*). Accordingly, reaction on metal-like sites rather than oxide or support sites is favored.

2. A model involving decomposition on the metal of a complex formed on the support is likewise consistent with most of the previous experimental observations (including those in this study) in regard to Peak *B*:

a. The increase in *A* and *B* areas with increasing reduction temperature (Table 3) is consistent with the reductive generation of new metal clusters accompanied by the sintering of these clusters to large, 3*D* crystallites which are sites for α-carbon hydrogenation (Reaction *A*), for spillover to the support of CO and atomic hydrogen, and for decomposition of the CH_xO species (Re-

action *B*) previously formed on the support from spilled-over CO and hydrogen. The increasing population of *B* sites with increasing extent of reduction argues against their assignment to cobalt or nickel aluminate since this phase is reduced to small metal clusters and any active sites on the aluminate would diminish as the extent of reduction is increased.

b. The increasing population of the *A* state (higher reaction rate for α-carbon hydrogenation) relative to the *B* state (CH_xO decomposition) with increasing metal loading and increasing reduction temperature (Table 3) is easily explained by an increasing population of metal sites for CO dissociation to α-carbon leading to Reaction *A* while the population of sites on the support for CH_xO formation is fixed (*34*). In other words, while the concentration of metal sites available for decomposition of the CH_xO complex is increased, the reservoir for these complexes is nevertheless constant.

c. The very significant increase in the temperature maximum of Peak *B* (decrease in the rate of Reaction *B*) with increasing reduction temperature (Table 3) could be explained by a lowering of the surface diffusion rate of the CH_xO complex over the support to metal crystallites due to progressive modifications of the support, e.g., support dehydroxylation as reduction temperature is increased. Indeed, Sen and Falconer (*34c*) postulate that decomposition on the metal of the CH_xO complex formed on the support is limited by surface diffusion to the metal. A recent study of CO hydrogenation on carbonyl-derived Fe/Al_2O_3 catalysts in this laboratory (*12*) indicates that catalyst activity is very significantly affected by the support dehydroxylation temperature.

d. The observation that Reaction *B* is favored by CO adsorption in the presence of hydrogen (*26, 27, 34*) (Fig. 3) is also consistent with a model involving formation of a "CO–H" complex. The previous observations by IR of a formate species on the Al_2O_3 surface of Ni/Al_2O_3 catalysts (*33, 39*) and on Co/kieselguhr catalysts (*43*) during CO hydrogenation provides further support for the role of a CH_xO complex.

e. From observations in this and a previous study (*44*) that the population of so-called "*B* sites" (sites for methoxy formation) or of the *B* reaction state (state for decomposition of methoxy species) is diminished but not completely removed by room temperature oxygen exposure (Fig. 9), it would be tempting to conclude that Reaction *B* involves sites that are nonmetallic, especially since metallic sites for Reaction *A* were removed by this treatment; however, it is not unreasonable to postulate that small metal clusters either partially buried in or surrounded by an oxide layer might be resistant to oxidation at low temperatures but nevertheless effective for CH_xO decomposition. These clusters might be less accessible to oxygen atoms because of the surrounding metal oxide phase and because ensembles required for oxygen dissociation might be present only in low concentration. That small cobalt clusters supported on Al_2O_3 are indeed inaccessible to oxygen at room temperature was confirmed recently by Neubauer (*45, 46*), who observed using Co^{57} Mössbauer emission spectroscopy that reduced superparamagnetic Co metal in 1 and 3% Co/Al_2O_3 was only partly oxidized by exposure to air at 298 K. Neubauer's catalysts were a pink color before reduction and a blue color after reduction; after exposure to air, they were the same blue color.

Reaction Mechanism of CO Hydrogenation on Co/Al_2O_3

The results of this study provide evidence that methanation occurs on Co/Al_2O_3 catalysts by two different mechanisms: (1) hydrogenation of α-carbon (Reaction *A*) and (2) decomposition of a CH_xO complex (Reaction *B*) formed on the support. Both reactions occur on metallic sites. Indeed the results in Fig. 1 and Table 3 show that both Peaks *A* and *B* (at about 435 and 500–

550 K, respectively) of 3–15% Co/Al_2O_3 reduced at normal temperatures lie within or below the typical operating temperature range for FT synthesis methanation on cobalt of 475–575 K.

The combined TPSR/TPD data in Fig. 9 show that molecularly adsorbed CO which is typically desorbed at temperatures from 373 to 473 K (*35, 47, 48*) and certainly below 650 K (*35, 47, 49*) (see peaks at 500 and 623 K for the TPD curve after TPSR to 373 K in Fig. 9a) is no longer present on the catalyst surface after TPSR in hydrogen at 398 K and higher; the CO desorption peak observed at 800–850 K in Fig. 9a is assigned with reasonable certainty to recombination of carbon and oxygen atoms on the surface (*35, 48, 49*). In other words, in the presence of hydrogen, CO adsorbed on Co/Al_2O_3 is completely dissociated at temperatures above 398 K; moreover a portion of the carbon thus formed is present on the surface in atomic form and can be desorbed by recombination at higher temperatures. This conclusion is further supported by the CO_2 TPD spectra in Fig. 9b showing that only a negligible amount of CO_2 desorbs at temperatures above 398 K confirming the absence of CO to combine with atomic oxygen under these conditions. Accordingly, it is clear that since adsorbed CO is completely dissociated above 398 K, methanation via Reaction *A* (which occurs well above 398 K) involves reaction of hydrogen with adsorbed carbon species from CO dissociation. This is further confirmed by the TPSR results after adsorption of CO at 523 K (Fig. 4) showing that the most important reaction peak has a maximum at 373 K, a distinct characteristic of adsorbed, atomic carbon commonly referred to as α-carbon (*37, 38*). The other peaks in Fig. 4 are easily assignable to β-carbon and other less active, polymeric carbon forms (*37, 38*) and the decomposition of the CH_xO complex. It should be emphasized that the peak for reaction of α-carbon with hydrogen occurs at a lower temperature than Peak *A* because, once formed, α-carbon is more reactive with hydrogen than is CO which dissociates first at about 425 K. The dissociation process thus determines the peak position for State *A*.

The facts that (1) CO is completely dissociated on Co/Al_2O_3 above about 400 K and (2) methanation via Mechanism *A* clearly involves reaction of hydrogen with carbonaceous species have important mechanistic implications. This suggests that the rate-determining step in CO hydrogenation on Co/Al_2O_3 at low reaction temperatures (475–525 K) involves carbon hydrogenation. This conclusion is contrary to that of Huang and Schwarz (*31*) who postulated that CH_x hydrogenation is rate-determining for Peak *A* while CO dissociation is rate determining for Peak *B* of Ni/Al_2O_3. Their conclusion was based on the assumption that CO adsorbed on the "*B* sites" did not dissociate until the reaction temperature of 550 K had been reached. In view of the similarity of the kinetic parameters for Co/Al_2O_3 and Ni/Al_2O_3 and the TPSR/TPD results of this study, we think their assumption is probably not correct. However, it should be emphasized that the rate-determining step may shift with changes in reactant concentrations, surface coverages, temperature, and conversion; accordingly one must be very cautious about generalizing what step may be rate-determining in CO hydrogenation or any other reaction. Nevertheless, the concept of Peak *B* corresponding to a decomposition of a CH_xO complex is quite consistent with the results of Huang and Schwarz (*31*).

Moreover, their interesting concept of different rate-determining steps (for two different sites) leads us to a similar concept—namely that of methanation via Reaction *B* being the "rate-dominating" step under certain reaction conditions because of its higher activation energy (the terminology "rate-controlling" is probably not applicable to a parallel process such as this). Indeed, a careful examination of the peak temperatures in Fig. 1 and Table 2 reveals that if methanation were conducted

on 3% Co/Al_2O_3 in the temperature range 450–525 K above the peak temperature for *A* and below that for *B*, the overall rate would be representative of reaction via Reaction *A*. However, at temperatures well above 550–575 K, Reaction *B* could dominate because of its higher activation energy. Accordingly, one would predict a shift to a higher activation energy with increasing reaction temperatures on a given catalyst and a shift to progressively higher activation energies with increasing metal loading and decreasing reduction temperatures, since the maximum for Peak *B* occurs at progressively lower temperatures as metal loading increases and reduction temperature decreases (see Fig. 1 and Table 3). In fact, Bartholomew *et al.* (*6–8*) observed increasing values of the activation energy for steady-state CO hydrogenation on Co/Al_2O_3 with increasing metal loading. Moreover, the activation energies for 3 and 10% Co/Al_2O_3 were found to be 87 and 112 kJ/mol (*8*), values close to the activation energies of 81 and 98 kJ/mol for Reactions *A* and *B*, respectively, suggesting that in the temperature range of the study (*8*) Reaction *A* dominated for the 3% Co while Reaction *B* dominated or at least became more important for the 10% Co catalyst.

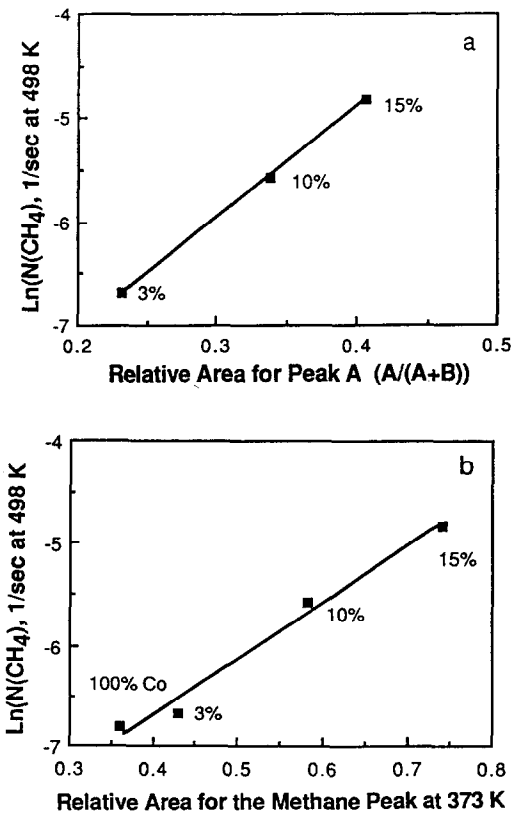

FIG. 10. (a) Log of turnover frequency for methane formation at 498 K during CO hydrogenation on Co/Al_2O_3 catalysts reduced at 698 K vs relative area of Peak *A* shown in Fig. 1. (b) Log of turnover frequency for methane formation at 498 K during CO hydrogenation on Co/Al_2O_3 catalysts reduced at 698 K vs relative area of Peak α due to α-carbon shown in Fig. 4.

While the principle that activation energies in complex supported systems will be influenced by the distribution of sites and the reaction temperature relative to the peak temperatures for reaction on those sites is probably a general one, the reader is cautioned that extrapolation of the specific trends observed for Co/Al_2O_3 and Ni/Al_2O_3 prepared by impregnation is not warranted. Several previous studies (*6–8, 26–32, 34, 35*) demonstrate that the adsorption and activity/selectivity properties of supported Co and Ni are strongly a function of support and preparation method. For example, only Peak *A* is observed on silica-supported Co and Ni (*27, 35*). Moreover, the steady-state activation energy of 3% Co/Al_2O_3 prepared by carbonyl decomposition on a highly dehydroxylated support increases with increasing reduction temperature (*8*) while the opposite trend is predicted for the catalysts of this study prepared by impregnation with an aqueous nitrate solution.

The results of this work show that Reaction *A* dominates at lower reaction temperatures. Accordingly, one might expect a correlation between steady-state activity under these conditions and the population of the *A* state in a series of Co/Al_2O_3 catalysts. This correlation is indeed well-observed in Fig. 10a where the turnover frequencies for CO hydrogenation on Co/Al_2O_3 at 498 K (*6, 7*) are plotted against relative areas of Peak *A* for three of the catalysts of this study. Further, if the reaction occurs by hydrogenation of α-carbon,

there should be a good correlation of the steady-state activity with the population of the species causing methane formation at 373 K after adsorption of CO at 523 K. Indeed this is observed in Fig. 10b for four of the catalysts of this study including unsupported cobalt. This provides further evidence that the methanation via Mechanism *A* occurs through the hydrogenation of adsorbed atomic carbon created by previous CO dissociation. Similar correlations between activity and dissociated carbon monoxide or α-carbon were found earlier for CO hydrogenation on Fe/Al_2O_3 catalysts (*50*) and Ru/SiO_2 (*51*) catalyst.

In Fig. 2, peak temperatures for *A* and *B* shift slightly up and down, respectively, with increasing CO coverage. The shift in Peak *A* to higher temperatures is consistent with reported kinetics of CO hydrogenation on cobalt (*25*) showing adsorbed CO to inhibit the reaction rate. The shift of Peak *B* to lower temperatures is probably due to a lower coverage of hydrogen with increasing CO coverage; decomposition of the methoxy is possibly inhibited by adsorbed hydrogen (*52*).

The Variation of Activity of Co/Al_2O_3 with Metal Loading and Dispersion and Its Basis

Two previous studies in this laboratory (*6, 8*) showed that the steady-state activity of Co/Al_2O_3 varies over 2–3 orders of magnitude with variations in metal loading, dispersion, and preparation; generally a trend of increasing activity with increasing metal loading and decreasing dispersion was observed. Kellner and Bell (*2*) observed a similar trend for Ru/Al_2O_3 catalysts, ascribing it to a decrease in the fraction of sites present on more active planar versus less active edge sites with increasing dispersion; Fu and Bartholomew (*8*) explained their results for Co/Al_2O_3 in a similar way.

However, recently obtained results for CO hydrogenation on Co overlayers on single-crystal W, Co/Al_2O_3 catalysts, and Fe/Al_2O_3 catalysts (*12–15*) provide convincing evidence that initial and steady-state rates on these surfaces are clearly independent of surface structure. Two recent studies (*12, 15*) provide new evidence that the variations in activity with metal loading and dispersion are strongly related to the extent of reduction of the catalyst; if the extent of reduction of Co/Al_2O_3 or Fe/Al_2O_3 is held constant, activity is independent of both metal loading and dispersion.

The results of this study provide a basis for explaining this phenomenon. They show that the activity of Co/Al_2O_3 catalysts is determined by the distribution of *A* and *B* states (reactions) and the reaction temperature with respect to the peak temperatures for these two sites. At low reaction temperatures, Reaction *A* predominates (as discussed above) and thus the activity of $cobalt/Al_2O_3$ catalysts correlates well with the population of *A* (see Fig. 10a) which clearly varies with metal loading and extent of reduction (see Table 3).

What accounts for the large variations in the relative area for Peak *A* (Fig. 10a) as a function of metal loading and for the negligible activity and absence of α-cabon on 1% Co/Al_2O_3? It should be emphasized that the 1% Co/Al_2O_3 catalyst adsorbs hydrogen (*5, 6*) (Table 1), although the adsorption is very highly activated (*23, 25*); further, it adsorbs CO at 298 K, albeit molecularly (*35, 47*); moreover, it does not dissociate CO during CO TPD (*35, 47*). Recent evidence indicates that the highly activated hydrogen adsorption and decrease in CO binding energy are very probably due to decoration of the metal crystallites in alumina-supported metals (*25, 53*). The extent of decoration apparently increases with decreasing loading (*25*), thus accounting for the inactivity of 1% Co/Al_2O_3. Since the Al_2O_3 support is not reducible, the decoration of metals by Al_2O_3 does not occur by migration during the reduction process as with titania-supported systems but rather may occur by dissolution of Al_2O_3 during impregnation (*54*) or decomposition of the metal aluminate during reduction (*32*).

Figure 1 shows that the Peak *B* tempera-

ture decreases with increasing metal loading. Assuming that Peak *B* corresponds to decomposition of the methoxy species on the metal, this observation might be explained by a higher density of metal crystallites in the higher loading catalysts and hence a shorter path for surface diffusion of the methoxy species from the support to the metal. In the case of the 1% Co/Al_2O_3 catalyst reduced to 1023 K, Peak *B* was observed at a very high temperature (about 773 K) consistent with this hypothesis. The fact that no *A* or *B* peak was observed on 1% Co/Al_2O_3 reduced at 873 K can be explained by the hypothesis that relatively large, undecorated crystallites may be necessary for spillover and formation of the methoxy complex; this suggests the possibility that a precursor to the methoxy species involving dissociated or partially activated CO and hydrogen atoms, e.g., a COH complex, is formed initially on the large, undecorated crystallites and then spills over to the support where it then forms the CH_3O (methoxy) species. Independent of a mechanism for the methoxy formation, it is clear that Peak *B* does not form in the absence of Peak *A*; moreover, the work of Falconer *et al.* clearly indicates that (1) formation of the methoxy species is an activated process, i.e., the amount formed increases with increasing temperature up to 385 K and hence the population of the *B* state increases as the adsorption temperature for CO increases from 300 to 385 K; and (2) the methoxy species is only formed in the presence of hydrogen but is more likely to decompose in the absence of hydrogen (*34, 52*).

CONCLUSIONS

1. Two mechanisms for CO adsorption and hydrogenation operate on alumina-supported cobalt: (1) CO dissociation on the metal followed by hydrogenation of α-carbon (Reaction *A*) and (2) spillover of CO and H to the support where a CH_xO complex is formed followed by diffusion of the complex to metal crystallites where it decomposes (Reaction *B*). Both reactions take place on metal sites; Reaction *A* is favored on large, 3*D* crystallites while Reaction *B* apparently takes place on both large and fairly inaccessible small crystallites. The distribution of these reactions (states) is a function of metal loading and reduction temperature; the fraction of methane formed by Reaction *A* increases with increasing metal loading and extent of reduction.

2. Methanation via Reaction *A* takes place via CO dissociation followed by the subsequent hydrogenation of α-carbon. At low reaction temperatures, Reaction *A* predominates and hence determines the overall rate, while at high reaction temperatures Reaction *B* dominates the reaction rate because of its higher activation energy.

3. The observed dramatic variations in CO hydrogenation activity with variations in metal loading and dispersion observed on alumina-supported cobalt can be explained by a distribution of *A* and *B* states. Catalysts of higher loading and extent of reduction involve a higher fraction of the *A* state and are more active in CO hydrogenation. Moreover, the activity of the *B* state increases with increasing metal loading, further explaining the higher activity of high metal loading catalysts. A linear correlation is observed between the log of turnover frequency for methane formation at 498 K during steady-state CO hydrogenation on Co/Al_2O_3 catalysts and the relative population of α-carbon formed during CO adsorption at 523 K. This correlation and the variation of the fraction of the *A* state with metal loading can be explained in part, by decoration of metal crystallites which becomes progressively more important at low metal loadings and ultimately (as in 1% Co/Al_2O_3) prevents CO dissociation.

ACKNOWLEDGMENTS

The authors gratefully acknowledge financial support from the Department of Energy, Office of Basic Energy Sciences, Division of Chemical Sciences (Contract DE-AC02-81ER10855 and Grant DE-FG02-87ER13763), technical assistance by Mr. Richard Jones and Dr. Huo-Yen Hsieh, and useful comments on the manuscript by Professor John Falconer.

REFERENCES

1. Bartholomew, C. H., Pannell, R. B., and Butler, J. L., *J. Catal.* **65,** 335 (1980).
2. Kellner, C. S., and Bell, A. T., *J. Catal.* **75,** 251 (1982).
3. Jung, H.-J., Walker, P. L., Jr., and Vannice, M. A., *J. Catal.* **75,** 416 (1982).
4. Boudart, M., and McDonald, M. A., *J. Phys. Chem.* **88**(11), 2185 (1984).
5. Reuel, R. C., and Bartholomew, C. H., *J. Catal.* **85,** 63 (1984).
6. Reuel, R. C., and Bartholomew, C. H., *J. Catal.* **85,** 78 (1984).
7. Bartholomew, C. H., and Reuel, R. C., *Ind. Eng. Chem. Prod. Res. Dev.* **24,** 56 (1985).
8. Fu, L., and Bartholomew, C. H., *J. Catal.* **92,** 376 (1985).
9. MacDonald, M. A., Storm, D. A., and Boudart, M., *J. Catal.* **102,** 386 (1986).
10. Jones, V. K., Neubauer, L. R., and Bartholomew, C. H., *J. Phys. Chem.* **90,** 4832 (1986).
11. Lee, C., Schmidt, L. D., Moulder, J. F., and Rusch, T. W., *J. Catal.* **99,** 472 (1986).
12. Rameswaren, M., and Bartholomew, C. H., *J. Catal.* **117,** 218 (1989).
13. Johnson, B. G., Rameswaren, M., Patil, M. D., Muralidhar, G., and Bartholomew, C. H., *Catalysis Today*, in press.
14. Johnson, B. G., Berlowitz, P. J., Goodman, D. W., and Bartholomew, C. H., *Surf. Sci.* **217,** 13 (1989).
15. Johnson, B. G., Bartholomew, C. H., and Goodman, D. W., submitted for publication.
16. Kelley, R. D., and Goodman, D. W., *Amer. Chem. Soc. Div. Fuel Chem.* **25,** 43 (1980).
17. Kelley, R. D., and Goodman, D. W., *Surf. Sci.* **123,** L743 (1982).
18. Goodman, D. W., *Acc. Chem. Res.* **17,** 194 (1984).
19. Berlowitz, P. J., and Goodman, D. W., *Surf. Sci.* **187,** 463 (1987).
20. *a.* Chin, R. L., and Hercules, D. M., *J. Phys. Chem.* **86,** 360 (1982); *b.* Burggraf, L. W., Leyden, D. E., Chin, R. L., and Hercules, D. M., *J. Catal.* **78,** 360 (1982).
21. Topsøe, N., and Topsøe, H., *J. Catal.* **75,** 354 (1982).
22. Zowtiak, J. M., and Bartholomew, C. H., *J. Catal.* **82,** 230 (1983).
23. Zowtiak, J. M., and Bartholomew, C. H., *J. Catal.* **83,** 107 (1983).
24. Castner, D. G., and Santilli, D. S., *ACS Symp. Ser.* **248,** 39 (1984).
25. Bartholomew, C. H., "Hydrogen in Catalysis" (Zoltan Paal and P. Govind Menon, Eds.), Chaps. 5 and 20. Elsevier, Amsterdam, 1986.
26. Kester, K. B., and Falconer, J. L., *J. Catal.* **89,** 380 (1984).
27. Kester, K. B., Zagli, E., and Falconer, J. L., *Appl. Catal.* **22,** 311 (1986).
28. Huang, Y.-J., and Schwarz, J. A., *Appl. Catal.* **30,** 239 (1987).
29. Huang, Y.-J., and Schwarz, J. A., *Appl. Catal.* **32,** 45 (1987).
30. Huang, Y.-J., Schwarz, J. A., Diehl, J. R., and Baltrus, J. P., *Appl. Catal.* **36,** 163 (1988).
31. Huang, Y.-J., and Schwarz, J. A., *Appl. Catal.* **36,** 177 (1988).
32. Huang, Y.-J., Schwarz, J. A., Diehl, J. R., and Baltrus, J. P., *Appl. Catal.* **37,** 229 (1988).
33. Lu, Y., Xue, J., Li, X., Fu, G., and Zhary, D., *Cuihau Xuebao* **6,** 116 (1985).
34. *a.* Glugla, P. G., Bailey, K. M., and Falconer, J. L., *J. Phys. Chem.* **92,** 4474 (1988); *b.* Glugla, P. G., Bailey, K. M., and Falconer, J. L., *J. Catal.* **115,** 24 (1989); *c.* Sen, B., and Falconer, J. L., *J. Catal.* **117,** 404 (1989); *d.* Sen, B., and Falconer, J. L., *J. Catal.* **133,** 444 (1988).
35. Lee, W.-H., Ph.D. dissertation, Brigham Young University, 1988.
36. Redhead, P. A., *Vacuum* **12,** 203 (1962).
37. McCarty, J. G., and Wise, H., *J. Catal.* **57,** 406 (1979).
38. Bartholomew, C. H., *Catal. Rev. Sci. Eng.* **24,** 67 (1982).
39. Mirodatos, C., Praliaud, H., and Primet, M., *J. Catal.* **107,** 275 (1987).
40. Bell, A. T., *Catal. Rev. Sci. Eng.* **23,** 203 (1981).
41. Pannell, R. B., Ph.D. dissertation, Brigham Young University, 1978.
42. Yao, H. C., and Shelef, M., *J. Phys. Chem.* **78,** 2490 (1974).
43. Gupta, R. B., Viswanathan, B., and Sastri, M. V. C., *J. Catal.* **26,** 212 (1972).
44. Huang, Y.-J., and Schwarz, J. A., personal communication, 1987.
45. Neubauer, L. R., Ph.D. dissertation, Brigham Young University, 1986.
46. Neubauer, L. R., and Bartholomew, C. H., paper in preparation.
47. Lee, W.-H., and Bartholomew, C. H., in preparation.
48. Prior, K. A., Schwaha, K., and Lambert, R. M., *Surf. Sci.* **77,** 193 (1978).
49. Choi, J.-G., Rhee, H.-K., and Moon, S. H., *Appl. Catal.* **13,** 269 (1985).
50. Perrichon, V., Turlier, P., Barrault, H., Forquy, C., and Menezo, H. C., *Appl. Catal.* **1,** 169 (1981).
51. Winslow, P., and Bell, A. T., *J. Catal.* **86,** 158 (1984).
52. Robbins, J. L., and Marucchi-Soos, E., Paper presented at the 11th North American Catalysis Society Meeting, Dearborn, MI, May 7–11, 1989.
53. Raupp, G. B., and Dumesic, J. A., *J. Catal.* **96,** 597 (1985); **97,** 85 (1986).
54. Wheeler, M. A., and Bettman, M., *J. Catal.* **40,** 124 (1974).